The Electrochemical Preparation and Kinetic and Product Studies of Acylated Quinol and Quinol Ether Imines. In Search of the Hydrolysis Products of the "Ultimate" Carcinogen of *N*-Acetyl-2-aminofluorene

Michael Novak,* John S. Helmick, Nicholas Oberlies, and Kanchugarakoppal S. Rangappa

Miami University, Department of Chemistry, 112 Hughes Hall, Oxford, Ohio 45056

William M. Clark and John S. Swenton*

The Ohio State University, Department of Chemistry, 120 West 18th Avenue, Columbus, Ohio 43210

Received September 22, 1992

The *N*-acetyl and benzoyl derivatives of 4-methoxy-4-phenyl-2,5-cyclohexadienone imine and the *N*-benzoyl derivative of 4-hydroxy-4-phenyl-2,5-cyclohexadienone imine (**1a–c**) have been prepared via anodic oxidation of the corresponding amide of 4-aminobiphenyl in either methanol or water/acetonitrile, respectively. The products and the kinetics of the acidic and basic hydrolyses of these compounds were studied and the results compared with other *N*-acylquinol imine derivatives, including *N*-acetyl-4-hydroxy-4-phenyl-2,5-cyclohexadienone imine (**1d**), generated by solvolytic routes. The chemistry of these compounds was dependent upon the pH and the substituents on the quinol imine derivative. The major reaction pathways were hydrolysis of the imine linkage to afford the respective dienone and phenyl migration to afford the amides of 2-hydroxy- or 2-methoxy-5-aminobiphenyl. The reactivity of the quinol imine derivatives follows the order: 4-hydroxyl more reactive than 4-methoxyl compounds and *N*-acetyl more reactive than *N*-benzoyl derivatives. The higher reactivity for the former compounds is attributed to the greater electron-donating ability of the 4-hydroxyl versus the 4-methoxyl group. The higher reactivity of the *N*-acetyl relative to the *N*-benzoyl derivatives is attributed to the ca. 30-fold increase in basicity of the *N*-acetyl functionality. The additive effect of the 4-hydroxyl and *N*-acetyl functionality on the basic quinol imine moiety makes compounds having both of the groups difficult to isolate in aqueous media. This serves as a limitation for the preparation of the quinol imine derivative of *N*-acetyl-2-aminofluorene via the anodic oxidation methods reported herein.

Quinol imines are hydrolysis products of the ultimate carcinogenic metabolites derived from biological oxidation of aromatic amines and amides.[1,2] Due to the instability of these materials, much of what is known about their chemistry is inferred from generation of the compounds in situ.[2,3] We were especially interested in preparing and isolating the *N*-acylquinol imine derivatives **1** and **2**. The preparation of **2** was of major interest since it has been implicated in the hydrolysis of *N*-(sulfonatooxy)-*N*-acetyl-2-aminofluorene, **3**,[2a,4] a putative ultimate carcinogenic metabolite of the well-known precarcinogen 2-(acetylamino)fluorene.[5] This compound has never been isolated, and its preparation may be problematical since it has an estimated half-life of a few minutes in aqueous solution at neutral pH and is also subject to rapid acid- and base-catalyzed decomposition.[2a] Thus, the preparation of the compounds **1a–d** and a study of their chemistry was investigated prior to initiation of research directed toward

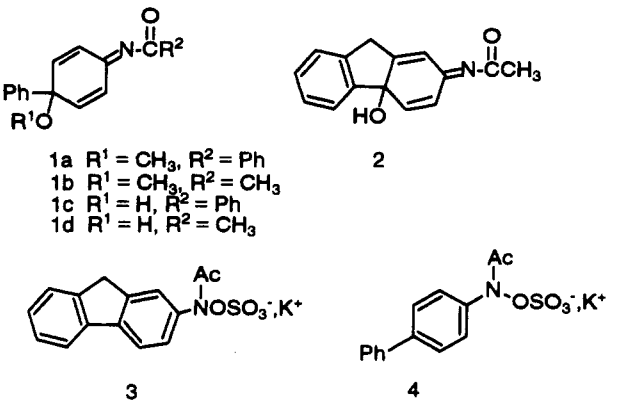

1a $R^1 = CH_3$, $R^2 = Ph$
1b $R^1 = CH_3$, $R^2 = CH_3$
1c $R^1 = H$, $R^2 = Ph$
1d $R^1 = H$, $R^2 = CH_3$

2

3

4

the preparation of **2** or its derivatives. We report herein anodic oxidation routes to **1a–c**, the products and kinetics of their acidic and basic aqueous hydrolysis, and a comparison of their chemistry with other *N*-acylquinol imines generated by solvolytic routes.[2,3] Notably, **1d** was detected during the hydrolysis of *N*-(sulfonatooxy)-*N*-acetyl-4-aminobiphenyl, **4**, a possibly carcinogenic metabolite of 4-(acetylamino)biphenyl.[6]

Anodic Oxidation Studies. Anodic oxidation of *p*-methoxyanilide derivatives serves as a general route to *N*-acylquinone imine derivatives as illustrated for the **5**

(1) For a general discussion, see: Lenk, W.; Rosenbauer-Thilmann, R. *Microsomes, Drug Oxidations, and Chemical Carcinogenisis*; Academic Press: New York, 1980; Vol. II.

(2) (a) Panda, M.; Novak, M.; Magonski, J. *J. Am. Chem. Soc.* **1989**, *111*, 4524–4525. (b) Novak, M.; Roy, A. K. *J. Org. Chem.* **1985**, *50*, 571–580.

(3) In contrast to quinol imine derivatives, a number of acylated quinol ethers have been prepared and some of their chemistry studied, i.e., *N*-acetyl-4-methyl-4-methoxy-*p*-benzoquinol imine: Gassman, P. G.; Granrud, J. E. *J. Am. Chem. Soc.* **1984**, *106*, 2448–2449 and references cited therein.

(4) Scribner, J. D. *J. Am. Chem. Soc.* **1977**, *99*, 7383–7384.

(5) DeBaun, J. R.; Miller, E. C.; Miller, J. *Cancer Res.* **1970**, *30*, 577–595. Weisburger, J. H.; Yamamoto, R. S.; Williams, G. M.; Grantham, P. H.; Matsushima, T.; Weisburger, E. K. *Cancer Res.* **1972**, *22*, 491–500.

(6) Kriek, E. *Chem.-Biol. Interactions* **1971**, *3*, 19–28. van de Poll, M. L. M.; Venizelos, V.; Meerman, J. H. N. *Carcinogenesis* **1990**, *11*, 1775–1781.

0022-3263/93/1958-0867$04.00/0 © 1993 American Chemical Society

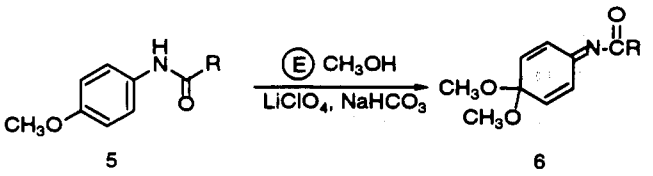

5 6

→ 6 conversion.[7] This type of anodic oxidation would provide **1a–d** if this chemistry could be extended to the amides of 4-aminobiphenyl. Anodic oxidation of **7a** in 5% aqueous methanol containing sodium bicarbonate with lithium perchlorate as supporting electrolyte was conducted at room temperature in a single-cell apparatus at a constant current of 0.3 amp. Workup and chromatography of the crude **1a** on silica gel led to partial hydrolysis to give 4-methoxy-4-phenyl-2,5-cyclohexadienone, which is very difficult to separate from **1a**. However, rapid chromatography on triethylamine-washed Florisil gave pure **1a** (80%). The structural assignment of **1a** was supported by ^1H NMR, ^{13}C NMR, and IR spectroscopy as well as its hydrolysis to the dienone mentioned above. The signal at δ 156 ppm in the ^{13}C NMR spectrum is especially indicative of the acylated imine carbon.

The acyl substituent on the amide has a marked influence on the isolated yield of the acylated quinol ethers in these oxidations. Whereas the benzoyl derivative **1a** was obtained in 80% yield from the anodic oxidation of **7a**, anodic oxidation of **7b** under the same conditions

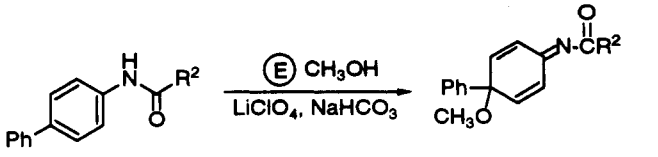

7a R^2 = Ph
7b R^2 = CH_3

1a R = Ph(80%)
1b R = CH_3(48%)

afforded the acetyl derivative **1b** in 48% yield. The lower yield of **1b** versus **1a** is probably not due to an inherent efficiency of the anodic oxidation chemistry. Rather, the acetyl derivatives are more subject to deacylation and imine hydrolysis under the reaction and isolation conditions. Whereas **1a** could be purified by chromatography on Florisil with virtually no hydrolysis to the dienone, rapid chromatography of crude **1b** on Florisil gave about 20% conversion to the dienone even under optimum conditions.

The successful synthesis of the *N*-acyl benzoquinol ether imines described above prompted further investigation into the anodic oxidation in aqueous solvents to prepare **1c** and **1d**. An extensive study of the variables in the anodic oxidation of anilides led to the following optimum conditions for conducting the reaction at room temperature: a 1:1:(6–9) mixture of dimethylformamide, water, and acetonitrile as solvent, a constant current of 0.15 A, 2% $LiClO_4$ as electrolyte, and $NaHCO_3$ as base. Under these conditions **7a** furnished, after chromatography on Florisil, **1c** (30%) in addition to **8c** (15%). The structure of the latter product was established by comparison with an authentic sample prepared from 2-hydroxybiphenyl, **9**, as shown below.

The yield for preparation of the hydroxy derivative **1c** is substantially lower than for the corresponding methyl

(7) Chen, C.-P.; Chou, C.-T.; Swenton, J. S. *J. Am. Chem. Soc.* **1987**, *109*, 946–948. Swenton, J. S.; Bonke, B. R.; Chen, C.-P.; Chou, C.-T. *J. Org. Chem.* **1989**, *54*, 51–58.

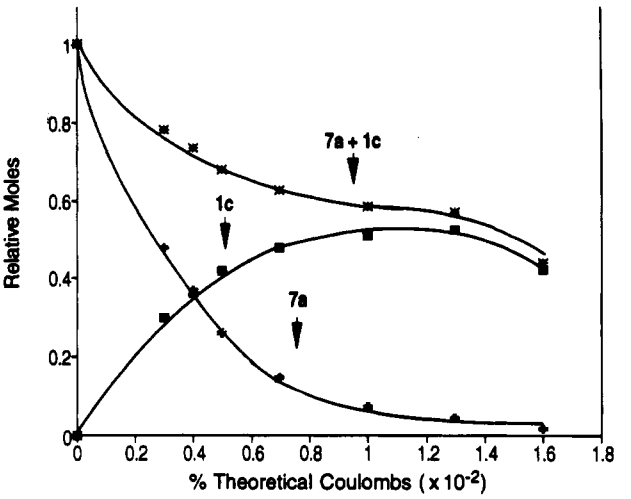

Figure 1. Relative yields of **1c** and **7a** as a function of Coulombs (the curves drawn are illustrative of the trend in yields and are of no theoretical significance).

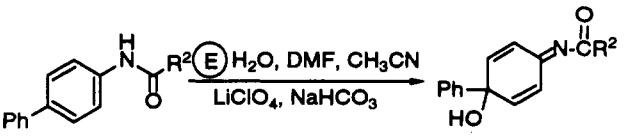

7a R^2 = Ph
7b R^2 = CH_3

1c R = Ph(30%)
1d ---

+

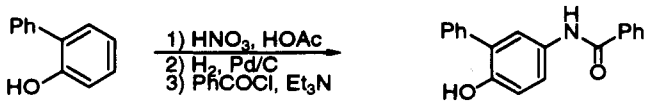

9 8c

ether **1a**. Although the lower yield is partially explained by formation of the aryl migration product noted above, the oxidation of **7a** warranted a more detailed study. The anodic oxidation of **7a** in aqueous media was monitored by high-pressure liquid chromatography to determine the current efficiency of the reaction and the extent of decomposition of **1c** during the electrochemical oxidation, isolation, and reaction workup.

The most apparent observation upon analysis of the graphical data given in Figure 1 is the efficient oxidation of starting amide, e.g., 92% consumption of **7a** at theoretical Coulombs. In addition, the rapid decrease in the sum of product and starting material in the first half-life of the reaction indicates that other uncharacterized reactions are competing with the formation of **1c**. Finally, the near constancy of the product yield between 80% and 130% of theoretical Coulombs suggests that the product is reasonably stable under the anodic oxidation conditions. However, complete conversion of the amide **7a** to the product **1c** does entail some loss of **1c** as suggested by the last point on the graph and the yield of **1c** (30%) when the preparative reaction was performed employing twice the theoretical amount of Coulombs. It appears that various factors may lower the yield of **1c**: competing electrochemical reactions, instability of the product at the latter stage of the reaction, and losses entailed by phenyl migration during the workup and isolation steps. *However, the important point is that anodic oxidation does furnish*

sufficient amounts of high purity material for product and kinetic studies.

All attempts to prepare the acetyl derivative **1d** under these as well as modified conditions (e.g., electrolysis in a divided cell) gave a complex mixture of products. The failure to isolate **1d** probably is not entirely a result of the anodic oxidation reaction itself but of the reactivity of the product (see below). The isolation of *N*-acylquinol derivatives such as **1d** is complicated not only by the hydrolytic stability of the acetyl linkage but also by a more facile phenyl migration. A substantial modification of the reaction conditions may be required to prepare derivatives akin to **1d** and **2**, and such studies are in progress.

Product Studies from Reaction of 1a–c in Aqueous Media. An understanding of the hydrolysis chemistry of **1** would be informative in developing conditions for preparation of **2** or its derivatives. The product studies and qualitative kinetic studies will be discussed herein, and detailed kinetic studies will be presented below. We wish to establish three points: (1) the products from basic hydrolysis, (2) the relative rate of phenyl migration in **1a** versus **1c**, and (3) the products of hydrolysis in mildly acidic and neutral aqueous solution. The basic hydrolysis of **1b** was studied under two sets of conditions. Stirring a solution of **1b** in acetonitrile/saturated sodium bicarbonate led to a slow reaction, affording after 10 days at room temperature a 92% yield of the dienone **10a**. These

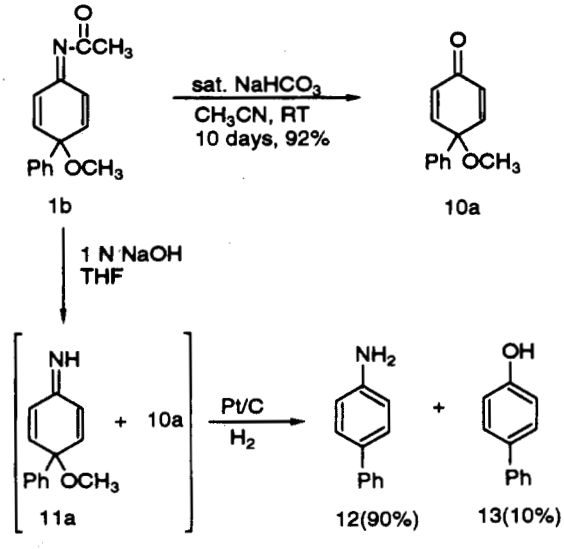

conditions, which mimic the basic conditions of the electrolysis, establish that the *N*-acetyl quinol ether imine derivatives are relatively stable to the solvent system used in the electrolysis. However, reaction of **1b** with aqueous sodium hydroxide at room temperature for 3 h led to formation of a new major product which could not be isolated without decomposition; therefore, the crude reaction mixture was hydrogenated. This led to the isolation of 4-aminobiphenyl, **12** (90%), and 4-phenylphenol, **13** (10%). A reasonable interpretation is that under basic conditions the fastest reaction is deacylation of the *N*-acylimine to form **11a**, followed by a slower hydrolysis of **11a** to the ketone **10a**.

As noted above, **8c** was a side product from the anodic oxidation of **1c**, and this would most reasonably result from a dienone–phenol-type rearrangement. To assess the relative facility of this rearrangement for **1a** and **1c**, simple kinetic studies were done in dry methylene chloride using trifluoroacetic acid (1.4×10^{-4} M) as catalyst. Under

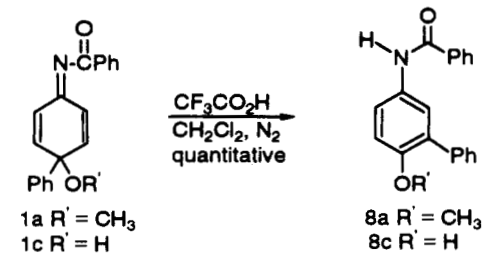

1a R' = CH_3
1c R' = H

8a R' = CH_3
8c R' = H

these conditions (see supplementary material for details), phenyl migration was the exclusive product, **1a** → **8a** and **1c** → **8c**, and **1c** was about seven times more reactive at 25 °C. As was suggested by the preparative studies, aryl migration catalyzed by adventitious acid is more facile for quinol derivatives (i.e., **1c**) than for quinol ethers (i.e., **1a**).

Hydrolysis of **1a–c** in acidic to neutral aqueous media [μ = 0.5 M (KCl), 5% CH_3CN, 20 °C] led to the ketones **10a,b**, the phenyl migration products **8a–c**, and the products of conjugate attack by H_2O followed by elimination of MeOH or H_2O, **14a** and **14b**.[2b,3] The identity of all products was confirmed by comparison to authentic materials. Details of the synthesis and characterization of authentic samples of these materials are presented in the Experimental Section; the pH dependence of these yields will be presented later.

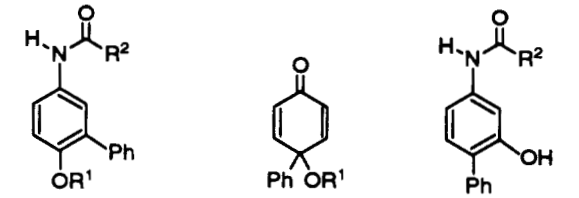

8a $R^1 = CH_3$, R^2 = Ph
8b $R^1 = CH_3$, $R^2 = CH_3$
8c R^1 = H, R^2 = Ph
8d R^1 = H, $R^2 = CH_3$

10a $R^1 = CH_3$
10b R^1 = H

14a R^2 = Ph
14b $R^2 = CH_3$

In Situ Generation of 1d. Although it was not possible to isolate **1d** from the anodic oxidation mixtures, the compound could be detected as a product of the hydrolysis of *N*-(sulfonatooxy)-*N*-acetyl-4-aminobiphenyl, **4**. Under the conditions employed in the kinetic studies described below, **4** decomposed with a pH- and buffer-independent rate constant of $3.8 \pm 0.6 \times 10^{-4}$ s^{-1}. In the pH range from ca. 6.0 to 10.0, it was possible to detect an intermediate in the hydrolysis of **4**, the decomposition of which was strongly acid catalyzed. The kinetics of the decomposition of this species were very similar to the authentic compounds **1a–c** (see below). This same intermediate could be detected by ^1H NMR (300 MHz) during the decomposition of **4** in deuterated 0.05 M 1/9 KD_2PO_4/K_2DPO_4 buffer, pD 8.90 (uncorrected) at 20 °C. Under these conditions, the half-life of **4** is ca. 0.5 h while the intermediate has a half-life of ca. 2.0 h. Much of the NMR spectrum of the intermediate is obscured by **4** and its own subsequent hydrolysis products, but three signals are clear: δ 6.35 (d, J = 10.1 Hz, 1 H), δ 6.79 (d, J = 10.1 Hz, 1 H), and δ 2.35 (s, 3 H). The cyclohexadienyl protons of authentic **1c** appear as two doublets at δ 6.42 (J = 9.9 Hz) and δ 6.82 (J = 9.9 Hz) under the same conditions, and the chemical shift of the acyl methyl group is in the range previously observed for other *N*-acetylquinol and quinone

imines.[2,3,8] This intermediate is assigned as **1d** on the basis of the NMR data, the reaction kinetics, and decomposition products **8d**, **10b**, and acetamide. Under the kinetic conditions, **1d** accounts for ca. 20% of the hydrolysis products of **4**, with 2-chloro-4-acetylaminobiphenyl, **15**, being the major product (ca. 65%). These two

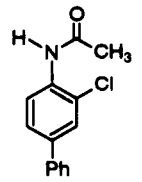

15

products are likely formed by competitive nucleophilic attack of H_2O and Cl^- on the nitrenium ion derived from heterolysis of the N–O bond of **4**.[2,9] A more detailed description of the hydrolysis behavior of **4** will appear elsewhere.[10]

Kinetics and Products of the Decomposition of 1a–d in Aqueous Solution. Kinetic measurements were performed by UV spectroscopy at 20 °C in the pH range 2–10 in 5% CH_3CN–H_2O at 0.5 M ionic strength (KCl). Initial concentrations of **1a–c** and **4** were ca. 2.0×10^{-5} M. The pH was maintained with HCl or buffers of $ClCH_2CO_2H$, CH_3CO_2H, KH_2PO_4, or tris [tris(hydroxymethyl)-aminomethane] (0.02–0.08 M total buffer). Buffer dilution experiments showed that significant buffer catalysis occurred only in tris buffers. Buffer-independent rate constants in tris buffers were obtained by linear extrapolation to zero buffer concentration. All other measurements were taken at 0.02 M total buffer concentration.

Over the entire pH range examined, **1a–c** exhibited clean pseudo-first-order or consecutive first-order reaction kinetics (see Experimental Section). All rate constants measured in this study are included in Tables III–VI in the supplementary material. One pH-dependent rate constant, k', could be observed over the entire pH range except for the most acidic solutions, in which the process governed by k' was too fast to measure. The other rate constant, k'', was also pH dependent and could be observed from pH 2.0 to 6.5. Plots of the logarithms of the buffer-independent rate constants vs pH are shown in Figure 2A for **1a,b** and Figure 2B for **1c,d**. The pH dependence of the two rate constants could be described by eqs 1 and 2.

$$k' = k_H'[H^+] + k_c' + k_{OH}'[OH^-] \quad (1)$$

$$k'' = k_H''[H^+] + k_c'' + k_{OH}''[OH^-] \quad (2)$$

Not all terms of these equations were observed for all three compounds. The rate constants derived from a weighted least-squares fit of the data to the two equations are reported in Table I. The quality of the fits, as shown in Figure 2, is good.

The rate constant for the decomposition of **4**, k_o, was buffer and pH independent at $3.8 \pm 0.6 \times 10^{-4}$ s^{-1}. At pH > 6.0 a second rate constant attributed to k' for **1d** was observed. It was not possible to observe **1d** below pH 6.0 because its rate constant for decomposition became greater than 10^2 larger than k_o, so **1d** never built up to appreciable concentrations. The data for k' for **1d** are included in Figure 2B, and the results of a fit of these data to eq 7 are presented in Table I. The k'' process was not observed in the limited pH range in which **1d** was detected.

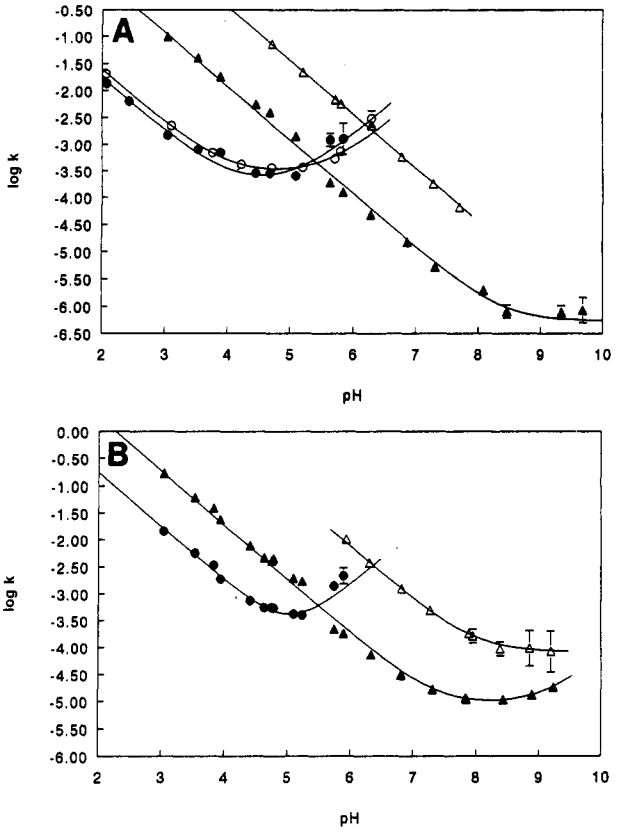

Figure 2. pH–rate profiles for **1a** in 5% CH_3CN–H_2O [μ = 0.5 M (KCl)] at 20 °C. The theoretical lines were calculated from eqs 1 and 2, and the kinetic data are reported in Table I. Triangles are for k'; circles are for k''. Error bars are indicated for all data points with an error > ± 0.1 log unit. (A) pH–rate profiles for **1a** (filled symbols) and **1b** (open symbols). (B) pH–rate profile for **1c** (filled symbols) and **1d** (open symbols).

Table I. Rate Constants Derived from Equations 1 and 2

	imine			
	1a	**1b**	**1c**	**1d**
$10^{-2}k_H'$ (M^{-1} s^{-1})	1.2 ● 0.1	36 ± 3	1.9 ± 0.1	75 ± 2
$10^6k_c'$ (s^{-1})	0.54 ± 0.04	*a*	8.3 ± 0.6	82 ± 6
$10^1k_{OH}'$ (M^{-1} s^{-1})	< 0.5[b]	*a*	6.2 ± 1.7	<50[b]
k_H'' (M^{-1} s^{-1})	1.7 ± 0.3	2.5 ± 0.3	18 ± 4	*c*
$10^4k_c''$ (s^{-1})	1.6 ± 0.4	2.6 ± 0.3	1.0 ± 0.5	*c*
$10^{-5}k_{OH}$ (M^{-1} s^{-1})	1.4 ± 0.4	0.7 ± 0.1	1.4 ± 0.7	*c*

[a] Reaction not monitored in the pH range where this process would be observed. [b] Upper limits based on observed rate constants at pH > 8.5 and error limits of these rate constants. [c] Not observed.

The data for **1d** are included in Figure 2B, and the results of a fit of these data to eq 7 are presented in Table I. The k'' process was not observed in the limited pH range in which **1d** was detected.

The rate constants of Table I and the data shown in Figure 2 indicate that although the reactivity patterns are similar for all four compounds, there are significant differences in the magnitudes of certain rate constants. *In particular, k_H' is much larger for the N-acetyl compounds **1b,d**, being 30-fold larger for **1b** than for **1a** and 39-fold larger for **1d** than **1c**.* The pH-independent process governed by k_c' also shows considerable variation among the three compounds for which it has been observed. There is significant error in k' for **1a,d** from data obtained in tris

(8) Novak, M.; Bonham, G. A.; Mulero, J. J.; Pelecanou, M.; Zemis, J. N.; Buccigross, J. M.; Wilson, T. C. *J. Am. Chem. Soc.* **1989**, *111*, 4447–4456.

(9) (a) Gassman, P. G. *Acc. Chem. Res.* **1970**, *3*, 26. (b) Gassman, P. G.; Hartman, G. D. *J. Am. Chem. Soc.* **1973**, *95*, 449 and references cited therein. (c) Pelecanou, M.; Novak, M. *Ibid.* **1985**, *107*, 4499–4503.

(10) Novak, M.; Helmick, J. S.; Eiger, E. To be submitted to *J. Am. Chem. Soc.*

buffers since the extrapolation process generated fairly large slopes and small intercepts with significant uncertainty for the buffer dilution plots. For this reason it is not possible to detect k_{OH}' with any reliability for these compounds. Upper limits for these rate constants are given in Table I. In general, k' is larger at all measured pH for the *N*-acetyl compounds compared to the corresponding *N*-benzoylimines and is also larger for the quinol imines compared to the corresponding quinol ether imines. In contrast, the pH-dependent and -independent components of k'' are much more similar for all three compounds for which they were observed.

The decomposition of **1c** in deuterated buffers was monitored by ^{1}H NMR spectroscopy to ascertain the chemistry associated with the k' and k'' processes. In 0.05 M 1:1 KD_2PO_4/K_2DPO_4 buffer, pD 7.36 (uncorrected) at 20 °C, **1c** disappears slowly with a half-life of ca. 10 h and is replaced by **8c** and **10b** with no evidence of an intermediate. Benzamide is also produced in a yield equivalent to that of **10b**. Under these conditions only the k' process can be observed by UV spectroscopy. In 0.05 M 1:1 AcOD/KOAc buffer and pD 5.18 (uncorrected) at 0 °C, **1c** disappears with a half-life of ca. 0.5 h. As it decomposes two intermediates are formed in its place. These decompose much more slowly into **8c**, **10b**, and benzamide. It appears that these intermediates are in equilibrium with **1c** after the initial phase of the reaction because **1c** can be detected at long reaction times at higher concentrations than predicted from its initial half-life of 0.5 h. The equilibrium constant for this process (**1c** ⇄ **16c**) appears to be ca. 2.0 from integration data taken at long reaction times. Most of the NMR spectra of these two species is obscured by **1c** at early reaction time, and the decomposition products at later reaction times, but the following signals could be assigned to two intermediates: δ 6.16 (d, J = 10.2 Hz) and δ 6.43 (d, J = 10.2 Hz); δ 6.14 (d, J = 10.2 Hz) and δ 6.40 (d, J = 10.2 Hz). The material with the doublets at δ 6.16 and 6.43 is produced in larger yield (ca. 2:1).

On the basis of the NMR data and the eventual decomposition products, as well as analogy to earlier studies,[2a,8] these materials are identified as the two diastereomeric amidocarbinols **16c**. Under the kinetic conditions in 1:1 acetate buffer, k' is ca. 8 times larger than k'', so k' describes the approach to equilibrium involving **1c** and **16c**, and k'' is apparently associated with the decomposition of these amidocarbinols. The UV spectroscopic data provided no indication of a third rate constant. If the two diastereomeric carbinols are in equilibrium with **1c**, this is expected, and k'' should be considered to be the weighted average of the decomposition rate constants of the two amidocarbinols, **16c**. At the higher pH the rapid base-catalyzed decomposition of **16c** (k_{OH}'' of Table I) will destroy the equilibrium between **1c** and **16c**, and the individual rate constants for the decomposition of the two amidocarbinols would, in principle, be observable. Since the k'' process is not experimentally observable above pH 6, it is not possible to detect these two rate constants.

The yields of the decomposition products of **1a–c** and **4** were monitored by HPLC on the same solutions used for the kinetics measurements. Yields in tris buffers were buffer dependent, so the buffer-independent yields were determined by extrapolation to zero buffer concentration.

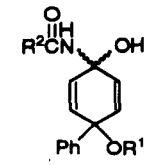

16a $R^1 = CH_3$, R^2 = Ph
16b $R^1 = CH_3$, $R^2 = CH_3$
16c R^1 = H, R^2 = Ph
16d R^1 = H, $R^2 = CH_3$

Their yields are reported in Tables VII–X in the supplementary material and are summarized graphically in Figure 3.

Figure 3A shows that the hydrolysis of the *N*-benzoylquinol ether imine, **1a**, yields predominantly the dienone **10a** and the phenyl migration product **8a**. The yields of both major products vary considerably with pH. The product of conjugate attack of H_2O followed by MeOH elimination,[2b,3] **14a**, is detectable but is only a minor reaction product in H_2O. Figure 3C shows that the major decomposition products of the *N*-benzoylquinol imine **1c** are **10b**, the phenyl migration product **8c**, and small amounts of **14a**.

The decomposition of **1b** under our reaction conditions yields **10a**, **8b**, and minor amounts of **14b** (Figure 3B). Under the kinetic conditions, decomposition products of **1d** account for only ca. 20% of the hydrolysis products of **4** as shown in Figure 3D. The major reaction product formed under all conditions is **15**. The variation in the yields of **10b** and **8d** with pH is very similar to that seen for **10b** and **8c** in Figure 3C. As in that case, **14b**, the isomer of **8d**, is formed in very low yield under some pH conditions. When the product studies were performed at lower Cl^- concentrations, the yields of the decomposition products of **1d** increased. A discussion of the variation in product yield with Cl^- concentration will be presented elsewhere.[10]

The amidocarbinols **16a–c** were observed by UV or NMR spectroscopy, and **16d** is assumed to be formed due to the overall similarity of the decomposition of **1d** to that of the other *N*-acylimines. The NMR data for **1c** and the HPLC data for the same compound, shown in Figure 4, require that **16c** be formed reversibly. The HPLC data show that the disappearance of **1c** at pH 4.01 and 4.78 is biphasic in nature. At each pH, about 60% of **1c** disappears rapidly at a rate consistent with k', and the rest decomposes more slowly at a rate consistent with k''. The amount of **1c** present at the end of the rapid initial step indicates that the equilibrium constant for **1c** ⇄ **16c** is about 1.5. At pH 5.64, k'' is larger than k' (Figure 2B), and the disappearance of **1c** takes on a first-order appearance. The rate of disappearance of **1c** at this pH is consistent with the magnitude of k'.

The mechanism of Scheme I provides a framework for understanding the kinetic data and the effect of pH on the yields of the major reaction products of **1a–d**. It provides for the reversible formation of **16a–d** under acidic pH conditions, the decomposition of **16a–d** into **10a,b** via acid- or base-catalyzed or uncatalyzed paths, the formation of the migration products from the N-protonated conjugate acids of **1a–d**, **17a–d**, and base-catalyzed and uncatalyzed pathways for the formation of the migration products. This mechanism is very similar to one proposed earlier to describe the hydrolysis of *N*-acetyl-*p*-benzoquinone imine, a reaction in which an amidocarbinol intermediate was

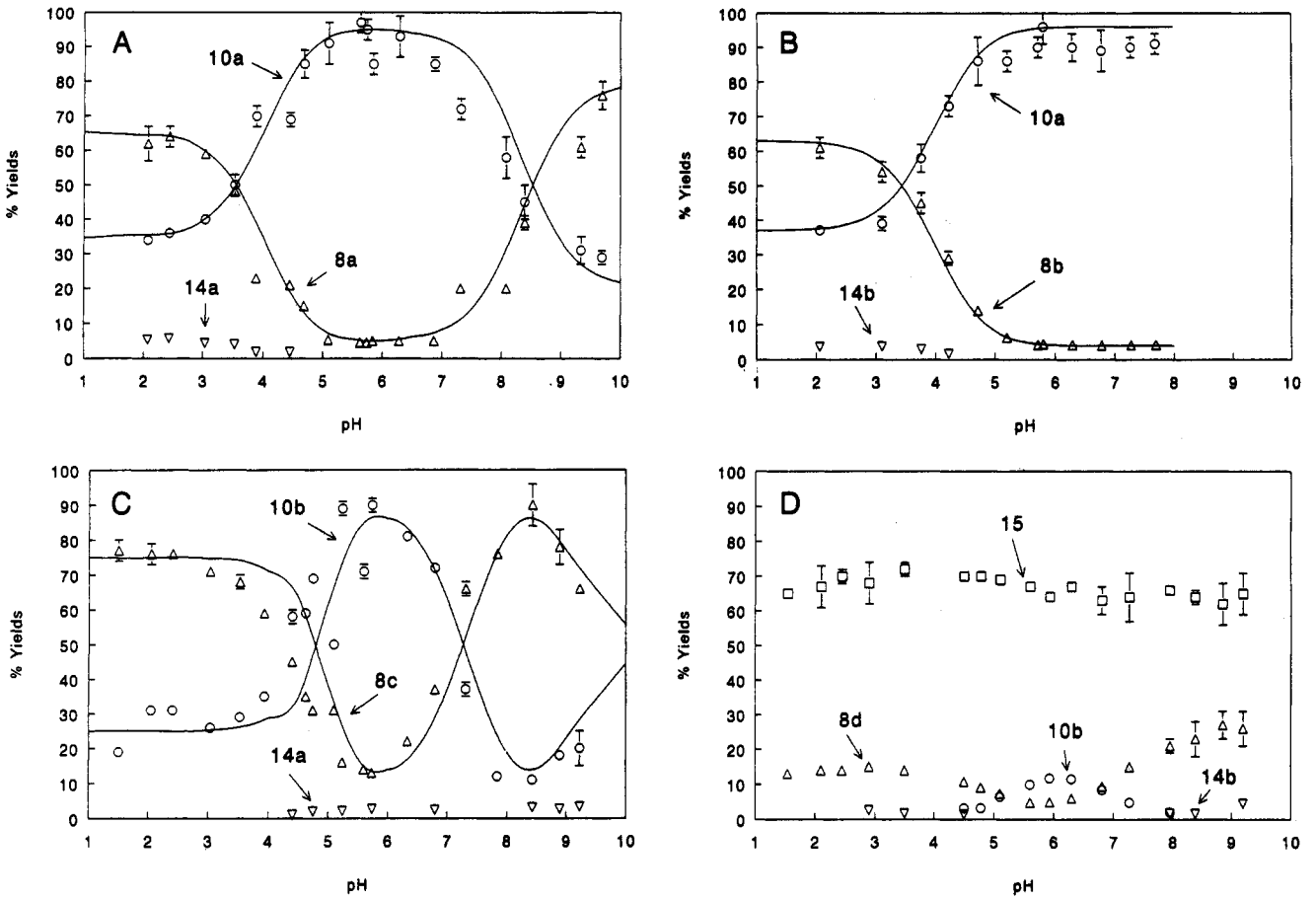

Figure 3. Product yields vs pH profile for **1a–c** and **4** under kinetic conditions. Error bars are included for all points with an error >±1%. Theoretical lines for **1a**, **1b**, and **1c** were derived from kinetic simulations which employed the data of Tables I and II. (A) Profiles for **1a**: circles = **10a**, triangles = **8a**, inverted triangles = **14a**. (B) Profile for **1b**: circles = **10a**, triangles = **8b**, inverted triangles = **14b**. (C) Profile for **1c**: circles = **10b**, triangles = **8c**, inverted triangles = **14a**. (D) Profile for **4**: circles = **10b**, triangles = **8d**, inverted triangles = **14b**, squares = **15**.

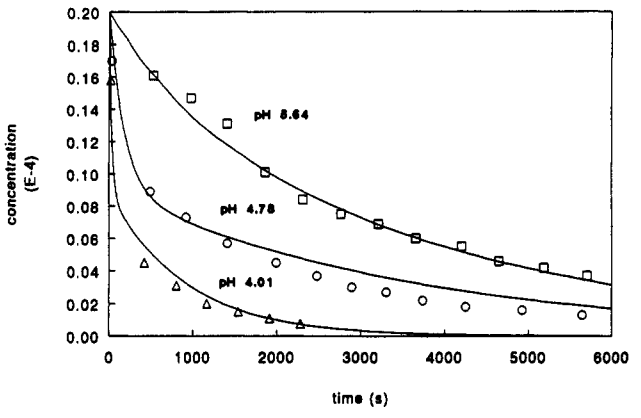

Figure 4. Plots of concentration of **1c** vs time obtained in 0.02 M acetate buffers at the indicated pH under conditions identical to those of the kinetic study. Initial concentration of **1c** was 2.0 × 10^{-5} M in all runs. Theoretical lines were calculated from kinetic simulations which employed the data of Tables I and II.

also observed.[8] Results of kinetic simulations for **1a,c** based on this mechanism are described below.

Kinetic Simulations. Analysis of the kinetic and product data for **1a,c** in terms of the mechanism of Scheme I requires estimates of the rate constants shown in Table II. Explanation of these assignments is given below.

pK_1 and pK_3. The pK_a of the conjugate acid of the *N*-benzylimine **19a** was determined by UV spectrophotometric titration under the reaction conditions to be 6.22 ± 0.08. The inductive effect upon the pK_a by substitution of a carbonyl for a methylene group α to the N is −5.4.[11] The C–N rotational barrier provides an approximation to

Scheme I. Hydrolysis of N-Acylated Quinol and Quinol Ether Derivatives

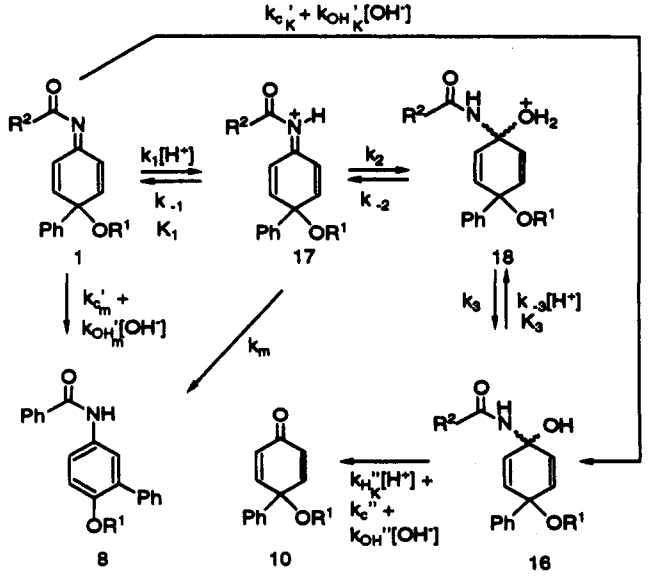

(11) Pracejus, H. *Chem. Ber.* **1959**, *92*, 988–998. Fersht, A. R. *J. Am. Chem. Soc.* **1971**, *93*, 3504–3515.

Table II. Microscopic Rate and Ionization Constants Used in the Kinetic Simulations

constant[a]	estimated values[b] 1a	1b	1c
pK_1	-3.7	-2.3	-3.7
k_1	1.2×10^7 M^{-1} s^{-1}	3.0×10^8 M^{-1} s^{-1}	1.2×10^7 M^{-1} s^{-1}
k_{-1}	6.0×10^{10} s^{-1} [c]	6.0×10^{10} s^{-1} [c]	6.0×10^{10} s^{-1} [c]
k_2	5.7×10^5 s^{-1}	6.9×10^5 s^{-1}	8.6×10^5 s^{-1}
k_{-2}	1.4×10^7 s^{-1}	9.6×10^6 s^{-1}	9.0×10^7 s^{-1}
k_m	3.0×10^4 s^{-1}	2.9×10^4 s^{-1}	8.6×10^4 s^{-1}
pK_3	-5.8	-5.4	-5.8
k_3	5.8×10^{11} s^{-1} [d]	5.8×10^{11} s^{-1} [d]	5.8×10^{11} s^{-1} [d]
k_{-3}	9.3×10^5 M^{-1} s^{-1}	2.3×10^6 M^{-1} s^{-1}	9.3×10^5 M^{-1} s^{-1}
k_{H_K}''	0.62 M^{-1} s^{-1}	0.96 M^{-1} s^{-1}	4.95 M^{-1} s^{-1}
k_{c_K}'	1.1×10^{-7} s^{-1}	[e]	
k_{c_m}'	4.3×10^{-7} s^{-1}	[e]	8.3×10^{-6} s^{-1}
k_{OH_K}'		[e]	3.1×10^{-1} M^{-1} s^{-1}
k_{OH_m}'		[e]	3.1×10^{-1} M^{-1} s^{-1}

[a] Defined in Scheme I. [b] Estimated as described in the text. Other rate constants necessary for the simulation are given in Table V. [c] See ref 13. [d] See ref 20. [e] Reaction not monitored under pH conditions in which this process would be observed.

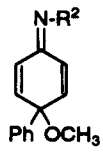

19a $R^2 = PhCH_2$
19b $R^2 = CH_3CH_2$

the resonance effect of the carbonyl group since that rotational barrier is lost on protonation at N.[11,12] We have previously estimated a rotational barrier of 6 kcal/mol for *N*-acetyl-*p*-benzoquinone imine.[8] If that value is used, the estimated pK_a's of **17a** and **17c** (pK_1) is -3.7. The difference in the inductive effects of OMe and OH in **17a,c** are minor, especially after attenuation through a vinyl group and methine carbon, so the same pK_a is used for both compounds. Perrin has measured the deprotonation rate constant for N-protonated acrylamide[13] at 6.0×10^{10} s^{-1}, and we have taken this value as an estimate of k_{-1}, fixing k_1 at 1.2×10^7 M^{-1} s^{-1}.

The pK_a of **20** is 13.05 ± 0.03.[8] If we assume $\rho_1 = -8.2$ ± 1.0 for the substituent effect of a group bonded to the central carbon of a tertiary alcohol,[14] then the pK_a for removal of the OH proton of **16a** is 11.2, based on σ_1 values of -0.05 for CH_3, 0.10 for Ph, 0.25 for C=O, 0.25 for OCH_3, and 0.27 for BzNH, and attenuation of the substituent effect through the vinyl group and methine carbon by a factor of 0.4 each.[15]

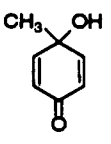

20

A similar correlation based on σ^* values and a ρ^* of -1.42 for the effect of a substituent on the ionization of a tertiary alcohol gives a pK_a of 12.2 for **16a**.[16,17] The average value of 11.7 was taken for the pK_a of **16a**. The same value is assumed for **16c**. This pK_a is 3.8 units lower than that of MeOH.[16] If the same substituent effect applies to the deprotonation of protonated alcohols,[18] then pK_3 for **18a,c** is -5.8, based on the pK_a of $MeOH_2^+$ of -1.98.[19] We chose k_3 to be 5.8×10^{11} s^{-1}, the rate constant for proton exchange between H_3O^+ and H_2O at 25 °C.[20] This fixes k_{-3} at 9.3×10^5 M^{-1} s^{-1}.

There are many sources of error in these estimates, and we have ignored differences in pK_a for the different diastereomers of structure **18**. The estimated errors in pK_1 and pK_3 are ±2 pK units. The errors in the diffusion-controlled rate constants k_{-1} and k_3 should be relatively small, so the errors in k_1 and k_{-3} are $\approx \pm 10^2$ M^{-1} s^{-1}.

***k*₂ and *k*ₘ.** The yield of the migration product **8a** derived from **1a** at pH 6.0 is ca. 5% (Figure 3A). At the same pH, the yield of **8c** derived from **1c** is ca. 9% (Figure 3C). Under these conditions, the amidocarbinols **16a,c** are irreversibly converted into **10a,b** by pH-independent and OH^--catalyzed routes (k_c'' and k_{OH}'') because the acid-catalyzed process which is responsible for the reversible formation of the amidocarbinols is very slow at this pH Table I. The k_c' and k_{OH}' terms have not yet contributed significantly to the overall reaction at this pH, so they can be ignored. The product yields under these conditions are governed by k_2 and k_m. The lack of general acid catalysis indicates that proton transfers are not rate limiting, so under these conditions k_H' is given to a first approximation by eq 3. The values of k_H' from Table I,

$$k_H' = k_1(k_2 + k_m)/k_{-1} \quad (3)$$

the estimate of pK_1, and the yields of the major reaction products **8a** and **10a** or **8c** and **10b** at pH 6.0 led to the estimates of k_2 and k_m given in Table II. The estimated error in both rate constants is $\pm 10^2$ s^{-1} for **1a,c**.

***k*₋₂ and *k*ₕₖ″.** The observed rate constant k_H'' consists of two parts: an acid-catalyzed component of the decomposition of **16** into **10** (k_{H_K}'') and the acid-catalyzed reversion of **16** which yields the migration product **8**. Again, since there is no evidence that proton transfers are rate limiting, k_H'' is given by eq 4. The contribution of the two

$$k_H'' = k_{H_K}'' + (k_{-3}k_{-2}k_m)[k_3k_2 + k_3k_m]^{-1} \quad (4)$$

terms of eq 4 to k_H'' can be determined from the product yields at pH 1–2 where the decomposition of **16** is dominated by k_H'' after correction for the small amount of the migration product initially formed in the more rapid k_H' step. Since all of the rate constants except k_{-2} in the second term of eq 4 have previously been estimated, the values of k_{H_K}'' and k_{-2} can be obtained. The error in k_{H_K}'' reported in Table II for **1a** and **1c** is relatively small at ±20%, but the error in k_{-2} is about the same magnitude estimated for k_2 and k_m.

***k*꜀ₖ′, *k*꜀ₘ′, and *k*ₒₕₘ′.** Above pH 6.0, the k_c' and k_{OH}' terms begin to contribute to the overall rate and product

(12) Perrin, C. L.; Johnston, E. R. *J. Am. Chem. Soc.* **1981**, *103*, 4697–4703.
(13) Perrin, C. L. *J. Am. Chem. Soc.* **1986**, *108*, 6807–6808.
(14) Fox, J. P.; Jencks, W. P. *J. Am. Chem. Soc.* **1974**, *96*, 1436–1449.
(15) Hansch, C.; Leo, A. *Substitution Constants for Correlation Analysis in Chemistry and Biology*; Wiley: New York, 1979; p 94. Charton, M. *J. Org. Chem.* **1964**, *29*, 1222–1227.
(16) Ballinger, P.; Long, F. A. *J. Am. Chem. Soc.* **1960**, *82*, 795–798.
(17) Perrin, D. D.; Dempsey, B.; Serjeant, E. P. *pKₐ Predictions for Organic Acids and Bases*; Chapman and Hall: London, 1981.
(18) Funderburk, L. H.; Aldwin, L.; Jencks, W. P. *J. Am. Chem. Soc.* **1978**, *100*, 5444–5459.
(19) Bonvicini, P.; Levi, A.; Lucchini, V.; Modena, G.; Scorrano, G. *J. Am. Chem. Soc.* **1973**, *95*, 5960–5964.
(20) Luz, Z.; Meiboom, S. *J. Am. Chem. Soc.* **1964**, *86*, 4768–4769.

distributions. In the absence of these terms, the yields of the reaction products would remain constant at their values near pH 6.0. For **1c** both terms are observed in the pH range in which product studies were done. The product data indicate that k_{c_m}' is the only contributor to k_c' for this compound and k_{OH}' contains equivalent contributions from k_{OH_K}' and k_{OH_m}'. Estimated errors in these terms are ±20%, and a small (ca. 10%) contribution of k_{c_K}' to k_c' cannot be ruled out by the available data. For **1a** only the k_c' term is important in the pH range in which product data were obtained. The contributions of k_{c_K}' and k_{c_m}' were determined from the product data. Again, we estimate an error of ±20% in these rate constants.

The comparison of the kinetic simulation results to the experimental data are shown in Figures 3A,C, and 4. In both cases the minor products, **14a,b**, which never account for more than ca. 5% of reaction products, were not included in the simulations. Figure 4 shows that the simulation predicts the biphasic nature of the plot of concentration of **1c** vs time at pH < 5.0 and also the transition to a first-order appearance at pH > 5.0. The quantitative agreement between the HPLC data and the simulation is quite good. The experimental data of Figure 4 is within $\pm 1.0 \times 10^{-6}$ M of that predicted by the simulation using a starting concentration of **1c** of 2.0×10^{-5} M.

The agreement between the observed and simulated product yields is quite good for **1a,c**. A significant part of the deviation in Figure 3A is due to errors in measurements of product yields by HPLC. In Figure 3C the agreement between observed and calculated yields is excellent except for the pH region between ca. 3.5 and 5.0. In this region, the product yields are critically dependent on the partitioning of the amidocarbinol **16c** between the two major products. The simulations oversimplify the real situation because there are really two diastereomeric amidocarbinols, each with a unique set of rate constants for formation and decomposition. A simulation including two amidocarbinols would make a better fit between calculated and experimental results in the pH range 3.5–5.0 because the two amidocarbinols could be made to decompose with somewhat different rate constants and with different product distributions. This was not pursued further since there was no experimental rate data to guide the simulation.

The equilibrium constants for the **1a** ⇄ **16a** and **1c** ⇄ **16c** conversions calculated from the simulation data are 5.1 and 1.2, respectively. We do not have any independent data for **1a**, but for **1c** this result is in accord with NMR and HPLC results discussed above. The mechanism of Scheme I invokes N-protonation of **1** in the first step of the acid-catalyzed reaction. An alternative mechanism involving protonation of the carbonyl oxygen has been considered for the hydrolysis of *N*-acetyl-*p*-benzoquinone imine.[8,21] Although that mechanism cannot be completely ruled out, substituent effects[8] and the results of ab initio calculations[21] suggest that it is less likely than the N-protonation mechanism. Detailed mechanisms for the steps represented by k_{c_K}', k_{OH_K}', k_{H_K}'', k_c'', and k_{OH}'' have been discussed for *N*-acetyl-*p*-benzoquinone imine and will not be considered here.[8]

The rearrangement processes represented by k_m, k_{c_m}', and k_{OH_m}' require some discussion. The acid-catalyzed reaction (k_1k_m/k_{-1}) is the *N*-acylimine analogue of the dienone–phenol rearrangement. The kinetic simulations indicate that k_1k_m/k_{-1} is ca. 3-fold larger for **1c** than for **1a**. This is in accord with our observation that **1c** undergoes phenyl migration ca. 7-fold faster than does **1a** in TFA/CH_2Cl_2. This rate acceleration for **1c** may be in the protonation step (k_1), the actual rearrangement process (k_m), or both steps. In the simulations we assumed that pK_1 for **1a** and **1c** are the same, but small substituent effect differences between OH and OCH_3 were ignored in making that assumption. In fact, σ^* values of 1.34 for OH and 1.81 for OCH_3 show that OH is somewhat more electron donating.[17] This could have an accelerating effect on both steps of the acid-catalyzed migration process.

The base-catalyzed migration (k_{OH_m}') was only observed for **1c** and probably occurs by the reaction sequence **1c** → **22** → **23**. This mechanism should also occur for **1d**, and

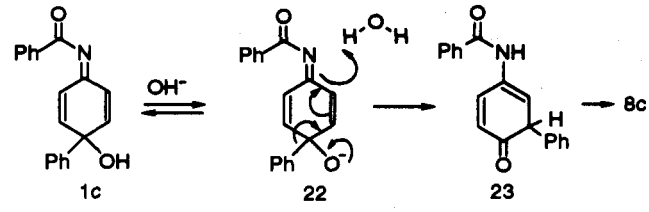

the failure to observe it may be due to errors in the rate constants measured in tris buffers discussed previously. This mechanism cannot occur for **1a** or **1b**, and no base-catalyzed process was evident for **1a** from either the kinetics or product data up to pH 10. The uncatalyzed process represented by k_{c_m}' appears to be more efficient for the quinol imines than for the quinol ether imines but is very slow in all cases and is only important near neutral pH.

For **1c,d** the minor amounts of **14a,b** found in the reaction mixtures may be formed by conjugate attack of H_2O and subsequent elimination of H_2O: **1c** → **24** → **14**.[2b,3]

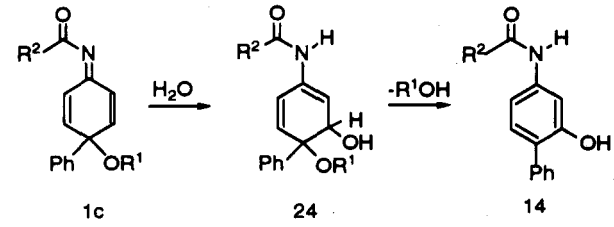

For **1a,b** these same two compounds must be formed by an addition–elimination mechanism. Due to the low yields of **14a,b** under all our reaction conditions, detailed mechanisms for their formation were not considered.

The reactivity differences among **1a–d** can be explained by substituent effect differences between OH and OCH_3 or CH_3CO and C_6H_5CO. *The greater electron-donating ability of OH compared to OCH_3 is responsible for the modest (2- to 10-fold) increases observed in k_H', k_c', and k_H'' (Table I) for **1c** compared to **1a** as discussed above with respect to the rearrangement process.*

The largest rate differences (30–39-fold) are observed in k_H' for the *N*-acetyl and corresponding *N*-benzoyl compounds (Table I). The pK_a values of the conjugate acids of the *N*-benzoyl- and *N*-ethylimines, **19a,b**, are 6.22 ± 0.08 and 7.65 ± 0.05, respectively, under the conditions of this study. *The (27 ± 5)-fold increase in basicity of **19b** compared to **19a** would be sufficient to explain most of the rate differences in k_H' for **1b** versus **1a** and **1d** versus **1c**, if the replacement of C=O for CH_2 has little*

(21) Novak, M.; Martin, K. A. *J. Org. Chem.* **1991**, *56*, 1585–1590.

effect on the differences in inductive substituent effects. In fact, the difference in σ^* for the benzyl and ethyl groups is 0.37, while the difference in σ^* for the benzoyl and acetyl groups is 0.39.[17] It appears that the differences in substituent effects of acetyl and benzoyl on K_1 of Scheme I are sufficient to account for most, if not all, of the rate differences observed in k_H'. The more modest differences in the components of k'' between **1b** and **1a** are consistent with the smaller differences in substituent effects on ionization equilibria or rate constants expected for AcNH and BzNH. For example, the effect of substitution of AcNH for BzNH on K_3 of Scheme I is calculated to be ca. 0.4-fold based on σ^* values of the two substituents and ρ^* of −1.42 for the effect of the substituent on the ionization.[16-18]

These considerations led to the estimates of pK_1 and pK_3 for **1b** shown in Table II. The overall rate constants for decomposition of **1b** (Table I) and the product data shown in Figure 3B were used to estimate the microscopic rate constants shown in Table II for **1b** as discussed above for **1a,c**. Figure 3B shows that the observed and predicted product yields for **8b** and **10a** are in good agreement in the pH range in which the measurements were made. Comparison of the microscopic rate constants derived for **1a** and **1b** shows that, within the limits of accuracy of the pK estimates, all rate constants for **1b** not associated with proton transfers are between 0.7 and 1.5 times their counterparts for **1a**. The equilibrium constant for **1b** ⇄ **16b** is 91 according to the simulations; this is 18-fold larger than for **1a** ⇄ **16a**. The protonation process described by K_1 is apparently primarily responsible for the difference. It was not possible to perform a similar simulation for **1d** due to our inability to detect **16d**.

Comparison with Other *N*-Acylquinol Imines. The chemistry of a limited number of *N*-acylquinol imines or their ether analogues has been investigated previously,[2,3] but only one of these materials, **21a**, was isolated.[3] The *N*-acetyl-4-methoxy-4-methyl-*p*-benzoquinolimine, **21a**,

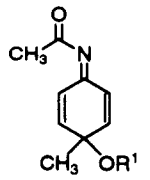

21a $R^1 = CH_3$
21b $R^1 = H$

and the corresponding hydroxy compound **21b**, undergo both methyl migration and conjugate addition of MeOH or H_2O and subsequent elimination.[2b,3] In contrast to **1a–d**, both **21a** and **21b** yield primarily the addition/elimination product under acidic conditions in MeOH or H_2O.[3,26] *The differences between **1a–d** and **21a,b** are probably due to the greater migratory ability of the phenyl group.*

The decomposition of **21b** in aqueous solution was investigated during a study of the hydrolysis of *N*-(sulfonatooxy)-*p*-acetotoluidide.[2b] The rate constant for acid-catalyzed decomposition of **21b** (k_H'), corrected to 20 °C, is ca. 5×10^3 M^{-1} s^{-1}, which is very similar to 7.5×10^3 M^{-1} s^{-1} observed for **1d**. The uncatalyzed decomposition of **21b** also occurs at about the same rate as **1d** under the same conditions. Both **1d** and **21b** yield significant amounts of the hydrolysis products **10b** and **20**, respectively. The pH dependence of the product yields for **21b** was studied less extensively than that of the compounds examined in this study, but the yield of **20** derived from **21b** follows the same general pattern observed here, for **10b**, reaching a maximum at pH of ca. 6.0–6.5 and decreasing at a pH more acidic or more basic than this.[2b] The decomposition of **21b** was not examined beyond pH 8, so the effects of any base-catalyzed decomposition of **21b** cannot be determined.

Summary. These results establish the order and origin of reactivity of N-acylated quinol imine derivatives in aqueous media. The higher reactivity of the *N*-acetyl versus the *N*-benzoyl compounds result primarily from the ca. 30-fold higher basicity of the imine nitrogen for the former derivatives. The slightly higher reactivity of the quinol versus the quinol ether (e.g., **1c** versus **1a**) results from the greater electron-donating ability of the OH versus the OCH_3 and thus the more facile aryl migration. The lower reactivity of the 4-methyl derivative, **21a**, versus the 4-phenyl compound, **1b**, probably results from the better migratory aptitude of phenyl relative to the methyl group. Although **1d** was not isolated, an intermediate detected in the reaction of **4** can be confidently assigned as **1d** based on the similarity of its rate constants for reaction to those of **1a–c** and a comparison of limited ^1H NMR data with that of **1c**. Finally, these results have allowed a comparison of the rate constants for reaction of the elusive **2**, detected in an earlier study,[2a] with the rate constants for **1a–d**. Under conditions identical to those used here, k_H', k_c', and k_{OH}' for **2** are 7.5×10^3 M^{-1} s^{-1}, 1.4×10^{-3} s^{-1}, and 1.5×10^2 M^{-1} s^{-1}, respectively. The acid-catalyzed rate constant, k_H', for **2** is identical to that observed for **1d**, but k_c' is 17-fold larger for **2** than for **1d**. *The reactivity of **2** in aqueous solution suggests that it will not be possible to isolate this material by the preparative methods described here. N-Benzoyl and/or methoxy analogues of **2** are more attractive synthetic targets based on the data available for **1a–d**.*

Experimental Section

General Procedures. ^1H NMR spectra in D_2O used DSS [3-(trimethylsilyl)-1-propanesulfonic acid, sodium salt] as standard. HPLC was performed on either a Microsorb C_{18} reversed-phase column using 8:2 MeOH/H_2O as eluant or on a μ-Bondapak C_{18} reversed-phase column using 6:4 or 7:3 MeOH/H_2O, buffered with 0.05 M 1:1 HOAc/KOAc, as eluant. HPLC peaks were monitored by UV absorption at 250 nm. All pH measurements were made at 20 ± 1 °C, and no corrections were applied to meter readings. Melting points are uncorrected.

All reagents and solvents used were reagent grade and used as obtained except as noted below. Tetrahydrofuran was purified by distillation from benzophenone ketyl, and dry CH_2Cl_2 was obtained by distillation from CaH_2 and then stored under N_2. The purification of H_2O and CH_3CN for kinetics has been described elsewhere.[2b,22] Dimethylformamide was dried by passing through a column of activated alumina followed by distillation under reduced pressure. Dry CH_3OH was obtained by distillation from $Mg(OCH_3)_2$. Potassium chloride and KH_2PO_4 were recrystallized from deionized H_2O and dried under vacuum. Potassium acetate, tris [tris(hydroxymethyl)aminomethane], and $ClCH_2CO_2H$ were used without further purification. Extractive workup refers to extraction of the material into the indicated solvent, washing the organic layer with a brine solution, drying over $CaSO_4$, concentration in vacuo, and drying to a constant weight under vacuum (1–2 Torr).

Preparative anodic oxidations were performed under constant current conditions in a single-cell apparatus (for more details,

(22) Novak, M.; Pelecanou, M.; Roy, A. K.; Andronico, A. F.; Plourde, F. M.; Olefirowicz, T. M.; Curtin, T. J. *J. Am. Chem. Soc.* **1984**, *106*, 5623–5631.

see ref 7). It is important that the sodium bicarbonate be freshly ground in a mortar and pestle and that heterogeneous reaction mixtures be efficiently stirred. The anode was a cylindrical platinum screen (5 × 3.5 mm in diameter, 50 mesh screen) and the cathode was a rectangular platinum sheet (8 × 8 mm).

***N*-Benzoyl-4-methoxy-4-phenyl-*p*-benzoquinol Imine, 1a.** *N*-Benzoyl-4-aminobiphenyl (1 g, 3.66 mmol), $LiClO_4$ (4.0 g), and $NaHCO_3$ (4.0 g) were added to a 5% H_2O/MeOH solution (300 mL), and the mixture was stirred vigorously for 20 min. The mixture was then anodically oxidized at a constant current of 0.3 A (6–7 V) at rt. The reaction was monitored by TLC (2% EtOAc/CH_2Cl_2) and was complete after 79 min (50% current efficiency). Filtration to remove insoluble $NaHCO_3$, addition of H_2O (100 mL), and extractive workup with CH_2Cl_2 (3 × 75 mL) gave the crude product as a yellow oil (1.2 g) which was dissolved in CH_2Cl_2 (10 mL) and impregnated on Florisil (3.0 g). Column chromatography on Florisil (10- × 2-cm column, 20% EtOAc/hexanes) was preceded by eluting Et_3N (2 mL) through the column. The product was isolated as a light yellow solid (880 mg, 80% yield), mp 88.0–90.0 °C. Analytically pure material was obtained after two recrystallizations (Et_2O/hexanes) as a white crystalline solid, mp 93.0–93.5 °C: IR (KBr) 1665, 1655, 1610, 1590, 1440, 1235, 1170, 1085, 1070, 1055, 1000, 830, 745, 730, 705, 690 cm^{-1}; ^1H NMR (200 MHz, $CDCl_3$) δ 7.97 (d, J = 7 Hz, 2 H), 7.6–7.3 (m, 8 H), 6.52 (AB q, $\Delta\nu$ = 14 Hz, J = 10 Hz, 4 H), 3.36, (s, 3 H); ^{13}C NMR (50 MHz, $CDCl_3$) δ 180.3, 155.7, 145.9, 139.5, 133.3, 133.0, 129.4, 128.7, 128.6, 128.1, 126.3, 125.7, 52.6 (one C not detected). Anal. Calcd for $C_{20}H_{17}O_2N$: C, 79.18; H, 5.65. Found: C, 79.20; H, 5.66.

***N*-Acetyl-4-methoxy-4-phenyl-*p*-benzoquinol Imine, 1b.** *N*-Acetyl-4-aminobiphenyl (0.25 mg, 1.0 mmol) in 5% H_2O/MeOH (200 mL) containing $LiClO_4$ (2.0 g) and $NaHCO_3$ (2.0 g) was anodically oxidized at 0 °C at a constant current of 0.15 A, and the progress of the reaction was followed by TLC (20% EtOAc/hexanes) and judged complete after 42 min (51% current efficiency). Workup and chromatography as detailed for **1a** gave first 4-methoxy-4-phenyl-2,5-cyclohexadienone, **10a** (R_f = 0.32, 20% EtOAc/hexanes), as a light yellow solid (20 mg, 10% yield), mp 88.0–90.0 °C (lit.[23] mp 91.0–92.5 °C, lit.[24] mp 85–87 °C), followed by a light yellow oil (138 mg, 48% yield) characterized as **1b** (R_f = 0.24, 20% EtOAc/hexanes): IR (neat) 2930 (w), 1690, 1660, 1610, 1450, 1355, 1210, 1080, 1065, 820, 750, 690 cm^{-1}; ^1H NMR (200 MHz, $CDCl_3$) δ 7.4–7.3 (m, 5 H), 6.47 (AB q, $\Delta\nu$ = 14 Hz, J = 10 Hz, 4 H), 3.36 (s, 3 H), 2.28 (s, 3 H); ^{13}C NMR (50 MHz, $CDCl_3$) δ 186.4, 150.5, 145.7, 139.6, 130.0, 128.6, 128.1, 125.9, 125.7, 52.6, 25.6; high-resolution MS m/e 241.1088, $C_{15}H_{15}NO_2$ requires 241.1099.

***N*-Benzoyl-4-hydroxy-4-phenyl-*p*-benzoquinol Imine, 1c.** *N*-Benzoyl-4-aminobiphenyl (500 mg, 1.84 mmol) was dissolved in DMF (30 mL) and added to a 10% H_2O/CH_3CN solution (300 mL). Lithium perchlorate trihydrate (4.0 g) and $NaHCO_3$ (4.0 g) were added, and the mixture was anodically oxidized at a constant current of 0.15 A (6–7 V) at rt. The reaction was monitored by TLC (25% EtOAc/hexanes) and was complete after 1.5 h (44% current efficiency). Workup as for **1a** gave a brown residue (490 mg) which was dissolved in CH_2Cl_2 (10 mL). Then Et_3N (5 mL) was added, and the residue was impregnated on Florisil (2 g) and column chromatography was performed as indicated above. The product **1c** (R_f = 0.35, 25% EtOAc/hexanes) was isolated as a light yellow oil which solidified upon addition of cold ether and scratching (170 mg), mp 105.0–107.0 °C. A recrystallization from Et_2O/hexanes gave a pale white solid (156 mg, 30%), mp 113.0–115.0 °C. Analytically pure material was obtained with an additional recrystallization, giving a white crystalline solid, mp 118.5–119.0 °C. A second compound was isolated as a light yellow solid (80 mg, 15% yield) and characterized as **8c** (R_f = 0.20, 25% EtOAc/hexanes). The spectral properties of **8c** were in agreement with authentically prepared material (below): IR (KBr) 3340, 1665, 1635, 1610, 1600, 1580, 1450, 1265, 1045, 945 cm^{-1}; ^1H NMR (200 MHz, DMSO-d_6) δ 7.87 (dd, J = 8, 1.5 Hz, 2 H), 7.7–7.6 (m, 1 H), 7.6–7.5 (m, 2 H), 7.4–7.3 (m, 5 H), 6.47 (AB q, $\Delta\nu$ = 98 Hz, J = 10, 4 Hz), 6.43 (s, 1 H); ^{13}C NMR (50 MHz, DMSO-d_6) δ 180.4, 156.7, 149.6, 142.2, 134.5, 133.6, 129.9, 129.8, 129.5, 128.5, 126.3, 122.5, 70.8. Anal. Calcd for $C_{19}H_{15}O_2N$: C, 78.87; H, 5.22. Found: C, 78.67; H, 5.22.

***N*-(Sulfonatooxy)-*N*-acetyl-4-aminobiphenyl, 4.** This material was prepared from *N*-hydroxy-*N*-acetyl-4-aminobiphenyl[25] by a method previously used to synthesize *N*-(sulfonatooxy)-*N*-acetyl-2-aminofluorene, **3**.[26] The crude product, obtained from the reaction performed with the *N*-hydroxy compound (0.42 mmol), was taken up into DMF (0.5 mL) and MeOH (1.0 mL) and precipitated with Et_2O (12 mL). After standing at 0 °C for several min, the white precipitate was collected by vacuum filtration and washed with dry Et_2O before being stored under vacuum at −25 °C in the presence of P_2O_5. Typically, 50 mg (ca. 35% yield) of material was obtained: ^1H NMR (300 MHz, DMSO-d_6) δ 2.30 (s, 3 H), 7.33 (tt, J = 1.2, 7.3 Hz, 1 H), 7.45 (t, J = 7.3 Hz, 2 H), 7.57 (AB q, $\Delta\nu$ = 19.6 Hz, J = 8.8 Hz, 4 H), 7.61–7.66 (m, 2 H); ^{13}C NMR (75.5 MHz, DMSO-d_6) δ 22.3 (CH_3), 122.6 (CH), 126.0 (CH), 126.5 (CH), 127.2 (CH), 128.9 (CH), 136.6 (C), 139.7 (C), 140.4 (C), 172.0 (C); high-resolution MS (FAB) m/e 383.9705, $C_{14}H_{12}NO_5SK_2$ requires 383.9705.

2-Hydroxy-5-nitrobiphenyl. 2-Hydroxybiphenyl (1.0 g, 5.9 mmol) was dissolved in glacial acetic acid (30 mL) in a 250-mL 3-necked, round-bottomed flask equipped with an addition funnel. The solution was then cooled in an ice bath to 10 °C, resulting in precipitation of some of the material. A solution of concentrated HNO_3 (0.34 mL, 5.9 mmol) and glacial acetic acid (5.0 mL) was then added slowly via addition funnel to the heterogeneous mixture, turning it bright orange. Upon completion, the ice bath was removed, and the solution was stirred vigorously at rt for 2.0 h. Saturated $NaHCO_3$ (200 mL) was then added, followed by extractive workup with CH_2Cl_2 (3 × 150 mL), giving a bright yellow sticky solid (1.2 g). Column chromatography on silica gel (15- × 1-cm column, 10% EtOAc/hexanes) first gave 2-hydroxy-3-nitrobiphenyl (R_f = 0.63, 20% EtOAc/hexanes) as a bright yellow solid (700 mg, 60% yield), mp 60.0–61.0 °C (lit.[27] mp 61.0–62.0 °C). The second compound isolated from the column was 2-hydroxy-5-nitrobiphenyl (R_f = 0.25, 20% EtOAc/H) as a bright yellow solid (400 mg, 40% yield), mp 124.0–125.0 °C (lit.[27] mp 124.0–125.0 °C).

***N*-Benzoyl-2-hydroxy-5-aminobiphenyl, 8c.** 2-Hydroxy-5-nitrobiphenyl (300 mg, 1.4 mmol) was placed in a 250-mL Paar hydrogenation bottle and completely dissolved in THF (40 mL). A 10% Pt/C catalyst (25 mg) was added, and the contents were placed under hydrogen (65 psi) for 3.0 h at rt. The mixture was then filtered through Celite, and the Celite was washed with additional THF (100 mL). After addition of Et_3N (0.2 mL, 1.5 mmol) to the combined THF solutions, a solution of benzoyl chloride (0.2 mL, 1.5 mmol) in THF (10 mL) was added slowly with stirring. A mildly exothermic reaction ensued with precipitation of a white solid. The mixture was heated on a steam bath to boiling for 15 min. After the mixture was cooled to rt, cold H_2O (300 mL) was added to the mixture, and the resulting white solid was filtered and washed twice with cold H_2O (10 mL). After drying, the white solid was used without further purification (250 mg, 62% yield), mp 188.0–189.0 °C: IR (KBr) 3250, 1645, 1625, 1530, 1505, 1490, 1410, 690 cm^{-1}; ^1H NMR (200 MHz, DMSO-d_6) δ 10.1 (s, 1 H), 9.5 (s, 1 H), 7.9 (d, J = 7.0 Hz, 2 H), 7.6 (d, J = 2.0 Hz, 1 H), 7.5–7.3 (m, 9 H), 6.9 (d, J = 9.0 Hz, 1 H); high-resolution MS m/e 289.1095, $C_{19}H_{15}NO_2$ requires 289.1099.

***N*-Benzoyl-2-methoxy-5-aminobiphenyl, 8a.** To a mixture of phenol **8c** (100 mg, 0.3 mmol), anhydrous K_2CO_3 (500 mg, 3.0 mmol), and dry THF (4.0 mL) was added excess CH_3I (1 mL). The reaction mixture was stirred vigorously at rt, and the reaction was monitored by TLC (20% EtOAc/hexanes). After 23 h, the mixture was filtered to remove K_2CO_3, and the solvent was removed under vacuum to give a white solid (**8a**) (110 mg, 95%

(23) Nillson, A.; Palmquist, Q.; Petterson, T.; Ronlon, A. *J. Chem. Soc.* **1978**, 696–707.

(24) Capparelli, M. P.; DeSchepper, R. E.; Swenton, J. S. *J. Org. Chem.* **1987**, *52*, 4953–4961.

(25) Maher, V. M.; Miller, E. C.; Miller, J. A.; Szybalski, W. *Mol. Pharm.* **1968**, *4*, 411–426.

(26) Beland, F. A.; Miller, D. W.; Mitchum, R. K. *J. Chem. Soc., Chem. Commun.* **1983**, 30–31. Smith, B. A.; Springfield, J. R.; Gutman, H. R. *Carcinogenesis* **1986**, *7*, 405–411.

(27) Vorozhtsov, N. N.; Troshchenko, A. T. *J. Gen. Chem. USSR (Engl. Transl.)* **1938**, *8*, 424.

yield), mp 189.0–190.0 °C: IR (KBr) 3250, 1640, 1520, 1480, 1400, 1225 cm^{-1}; ^1H NMR (200 MHz, $CDCl_3$) δ 7.9 (m, 3 H), 7.6 (dd, J = 8, 1.5 Hz, 1 H), 7.5–7.3 (m, 9 H), 6.9 (d, J = 8 Hz, 1 H), 3.8 (s, 3 H); high-resolution MS m/e 303.1272, $C_{20}H_{17}NO_2$ requires 303.1255.

***N*-Acetyl-2-hydroxy-5-aminobiphenyl, 8d.** This material was obtained by a procedure identical to that described for **8c**, except for the substitution of acetyl chloride for benzoyl chloride. The crude product was purified by chromatography on silica gel (3:1 CH_2Cl_2/hexanes), mp 158–160 °C (lit.[28] mp 160 °C): ^1H NMR (300 MHz, CD_2Cl_2) δ 2.11 (s, 3 H), 5.30 (s, br, 1 H), 6.90 (d, J = 9.4 Hz, 1 H), 7.16 (s, br, 1 H), 7.34 (dd, J = 2.7, 9.4 Hz, 1 H), 7.38 (d, J = 2.7 Hz, 1 H), 7.4–7.5 (m, 5 H); ^{13}C NMR (75.5 MHz, $CDCl_3$) δ 24.4 (CH_3), 116.2 (CH), 121.7 (CH), 122.7 (CH), 128.0 (CH), 128.4 (C), 129.0 (CH), 129.2 (CH), 130.9 (C), 136.7 (C), 149.5 (C), 168.2 (C).

***N*-Acetyl-2-methoxy-5-aminobiphenyl, 8b.** The material was prepared as indicated above for **8a**. Recrystallization from MeOH yielded the pure compound, mp 167–168 °C: IR (KBr) 3288, 1652, 1602, 1558, 1489 cm^{-1}; ^1H NMR (300 MHz, CD_2Cl_2) δ 2.11 (s, 3 H), 3.78 (s, 3 H), 6.93 (d, J = 8.8 Hz, 1 H), 7.29–7.42 (m, 5 H) 7.47–7.51 (m, 3 H); ^{13}C NMR (75.5 MHz, CD_2Cl_2) δ 24.5 (CH_3), 56.1 (CH_3), 111.9 (CH), 121.0 (CH), 123.3 (CH), 127.4 (CH), 128.3 (CH), 129.8 (CH), 131.2 (C), 131.8 (C), 138.5 (C), 153.6 (C), 168.4 (C); high-resolution MS m/e 241.1103, $C_{15}H_{15}NO_2$ requires 241.1103.

2-Hydroxy-4-nitrobiphenyl. 2-Amino-4-nitrobiphenyl was prepared from 2-bromo-5-nitrobenzoic acid as described in the literature.[29] This product was purified by recrystallization from benzene–petroleum ether, mp 70–71 °C (lit.[29b] mp 71–72 °C): ^{13}C NMR (75.5 MHz, $CDCl_3$) δ 109.5, 113.1, 128.3, 128.6, 129.2, 131.0, 133.3, 137.4, 144.5, 148.1. This material (160 mg, 0.75 mmol) was diazotized and converted into the phenol by a standard procedure.[30] The product was isolated from the reaction mixture by extraction into CH_2Cl_2 (3 × 5 mL). The extracts were combined and dried over Na_2SO_4. After concentration under vacuum, the product was purified by column chromatography on silica gel (3:1 CH_2Cl_2/hexanes) and finally by sublimation under vacuum. The phenol was obtained as a light yellow solid (100 mg, 62% yield), mp 90–93 °C. A previously reported mp of 200 °C appears to be in error,[31] and no other characterization was given in the earlier paper. Our material showed: ^1H NMR (300 MHz, DMSO-d_6) δ 7.35–7.45 (m, 3 H), 7.53 (d, J = 8.4 Hz, 1 H), 7.59 (m, 2 H), 7.73 (dd, J = 2.3, 8.4 Hz, 1 H), 7.77 (d, J = 2.3 Hz, 1 H), 10.7 (s, br, 1 H); ^{13}C NMR (75.5 MHz, $CDCl_3$) δ 111.2, 115.8, 128.8, 129.0, 129.5, 130.8, 134.8, 135.1, 148.1, 153.1; high-resolution MS m/e 215.0585, $C_{12}H_9NO_3$ requires 215.0582.

***N*-Benzoyl-2-hydroxy-4-aminobiphenyl, 14a.** This material was synthesized by the same procedure used for **8c** from 2-hydroxy-4-nitrobiphenyl (30 mg, 0.14 mmol). The crude product was purified by chromatography on silica gel (3:1 CH_2Cl_2/hexanes) to yield a grayish solid (31 mg, 76%), mp 86–87 °C: ^1H NMR (300 MHz, DMSO-d_6) δ 4.42 (s, 1 H), 6.62 (dd, J = 2.0, 8.1 Hz, 1 H), 6.69 (d, J = 2.0 Hz, 1 H), 7.13 (d, J = 8.1 Hz, 1 H), 7.2–7.35 (m, 8 H), 7.46–7.49 (m, 2 H), 9.8 (s, br, 1 H); ^{13}C NMR (75.5 MHz, DMSO-d_6) δ 115.3 (CH), 118.8 (CH), 125.9 (C), 126.6 (CH), 127.8 (CH), 127.9 (CH), 128.0 (CH), 128.9 (CH), 129.4 (CH), 130.5 (CH), 136.6 (C), 137.6 (C), 143.0 (C), 154.5 (C), 169.1 (C); high-resolution MS m/e 289.1102, $C_{19}H_{15}NO_2$ requires 289.1104.

***N*-Acetyl-2-hydroxy-4-aminobiphenyl, 14b.** This material was synthesized by the same procedure used for **8d** from 2-hydroxy-4-nitrobiphenyl (30 mg, 0.14 mmol). The crude product was purified by chromatography on silica gel (3:1 CH_2Cl_2/hexanes). The pure material was obtained as a fine white powder (25 mg, 79% yield), mp 229–230 °C: ^1H NMR (300 MHz, DMSO-d_6) 2.03 (s, 3 H), 6.98 (dd, J = 2.0, 8.3 Hz, 1 H), 7.15 (d, J = 8.3 Hz, 1 H), 7.24 (tt, J = 1.2, 7.2 Hz, 1 H), 7.35 (t, J = 7.6 Hz, 1 H), 7.42 (d, J = 2.0 Hz, 1 H), 7.50 (m, 2 H), 9.58 (s, 1 H), 9.90 (s, 1 H); ^{13}C NMR (75.5 MHz, DMSO-d_6) 24.1 (CH_3), 106.6 (CH), 110.3 (CH), 122.5 (C), 126.1 (CH), 127.8 (CH), 128.9 (CH), 130.2 (CH), 138.4 (C), 139.5 (C), 154.4 (C), 168.2 (C); high-resolution MS m/e 227.0945, $C_{14}H_{13}NO_2$ requires 227.0947.

***N*-Acetyl-3-chloro-4-aminobiphenyl, 15.** This material was prepared from *N*-acetyl-4-aminobiphenyl by N-chlorination with NaOCl, followed by rearrangement in warm HOAc/EtOH as described in the literature.[32] The crude product was recrystallized from EtOH/H_2O, mp 146.0–146.5 °C (lit.[32] mp 147 °C): ^1H NMR (300 MHz, CD_2Cl_2) δ 2.22 (s, 3 H), 7.3–7.45 (m, 3 H), 7.52 (dd, J = 2.2, 8.6 Hz, 1 H), 7.53–7.57 (m, 2 H), 7.65 (d, J = 2.2 Hz, 1 H), 7.66 (s, br, 1 H), 8.40 (d, J = 8.6 Hz, 1 H); ^{13}C NMR (75.5 MHz, CD_2Cl_2) δ 25.0 (CH_3), 122.0 (CH), 123.3 (C), 126.5 (CH), 127.0 (CH), 127.6 (CH), 128.0 (CH), 129.3 (CH), 134.3 (C), 137.9 (C), 139.5 (C), 168.5 (C).

***N*-Benzyl-4-methoxy-4-phenyl-*p*-benzoquinol Imine, 19a.** *N*-Benzoyl-4-methoxy-4-phenyl-*p*-benzoquinol imine, **1a** (72 mg, 0.24 mmol), was dissolved in THF (5 mL), benzylamine (0.03 mL, 0.26 mmol) was added, and the solution was stirred at rt. The reaction was monitored by TLC (20% EtOAc/hexanes) and was complete after 2.0 h. The reaction solvent was removed under vacuum, giving a yellow oil (100 mg) which was dissolved in CH_2Cl_2 and impregnated on Florisil (1.5 g). Chromatography on Florisil (10 × 2 cm column, gradient eluted from hexanes to 15% EtOAc/hexanes) was preceded by eluting Et_3N (2 mL) through the column. There was obtained a light yellow oil (56 mg, 82% yield) which was greater than 95% pure by ^1H NMR spectroscopy (200 MHz): IR (neat) 2932, 1602, 1583, 1489, 1449, 1069, 823 cm^{-1}; ^1H NMR (200 MHz, $CDCl_3$) δ 7.5–7.2 (m, 10 H), 6.9 (dd, J = 10, 2 Hz, 1 H), 6.6 (dd, J = 10, 2 Hz, 1 H), 6.3 (dd, J = 10, 2 Hz, 1 H), 6.2 (dd, J = 10, 2 Hz, 1 H), 4.9 (s, 2 H), 3.4 (s, 3 H); ^{13}C NMR (50 MHz, $CDCl_3$) δ 157.0, 143.0, 141.3, 139.8, 138.7, 133.6, 128.6, 128.4, 127.9, 127.7, 126.9, 125.7, 118.8, 77.6, 55.0, 52.2; high-resolution MS m/e 289.1471, $C_{20}H_{19}NO$ requires 289.1462.

***N*-Ethyl-4-methoxy-4-phenyl-*p*-benzoquinol Imine, 19b.** *N*-acetyl-4-methoxy-4-phenyl-*p*-benzoquinol imine, **1b** (110 mg, 0.44 mmol), was dissolved in THF (2 mL), ethylamine (0.02 g, 0.45 mmol) was added, and the solution was stirred at rt for 2 h. Workup and chromatography as for **19a** gave a light yellow oil (0.68 g, 68% yield) which was greater than 95% pure by ^1H NMR spectroscopy (200 MHz): IR (neat) 1601, 1579, 1489, 1447, 1089, 1073, 828, 756, 703 cm^{-1}; ^1H NMR (200 MHz, $CDCl_3$) δ 7.5–7.2 (m, 5 H), 6.8 (dd, J = 10, 2 Hz, 1 H), 6.52 (dd, J = 10, 2 Hz, 1 H), 6.45–6.15 (m, 2 H), 3.65 (q, J = 8 Hz, 2 H), 3.34 (s, 3 H), 1.32 (t, J = 8 Hz, 3 H); high-resolution MS m/e 227.1322, $C_{15}H_{17}NO$ requires 227.1310.

Kinetics. Kinetics of the decomposition of **1a–c** and **4** in aqueous solution were monitored in 5 vol % CH_3CN–H_2O at an ionic strength of 0.5 M maintained with KCl. HCl or buffers ($ClCH_2CO_2H$, AcOH, KH_2PO_4, Tris) were used to maintain pH. Total buffer concentrations ranged from 0.02 to 0.08 M. All kinetic measurements performed in aqueous solution were done at 20.0 ± 0.1 °C. General methods of preparing solutions and monitoring kinetics by UV methods have been described elsewhere.[2,8,22]

Concentrations of **1a–c** and **4** of ca. 2.0 × 10^{-5} M were used in the UV studies. These were obtained by injection of ca. 4 mM solutions (15 mL) of these compounds in dry DMF into the buffer solution (3 mL) which had been incubating in the thermostated sample compartment of the UV spectrophotometer. Changes in UV absorbance were monitored at 252 and 280 nm for **1a**, 254 nm for **1b**, 254 nm for **1c**, and 248 and 266 nm for **4**. Absorbance vs time data were fit to either the standard first-order rate equation or to the rate equation for two consecutive first-order processes (eq 5) by methods previously described.[2,8] The quality

$$A_t = A_1 e^{-k't} + A_2 e^{-k''t} + A_\infty \quad (5)$$

of these fits, judged by agreement between calculated and observed values of A_0 and A_∞, and by the standard deviations of the fits, is excellent.

(28) Burckhalter, J. H.; Tendick, F. H.; Jones, E. M.; Jones, P. A.; Holcomb, W. F.; Rawlins, A. L. *J. Am. Chem. Soc.* **1948**, *70*, 1363–1373.
(29) (a) Buckles, R. E.; Filler, R.; Hilfman, L. *J. Org. Chem.* **1952**, *17*, 233–242. (b) Forrest, J. *J. Chem. Soc.* **1960**, 566–573.
(30) Manske, R. H. F. In *Organic Syntheses*; Blatt, A. H., Gilman, H., Eds.; Wiley: New York, 1941; *Collect. Vol. I.*, pp 404–405.
(31) Finzi, C.; Mangini, A. *Gass. Chim. Ital.* **1932**, *62*, 664–677.
(32) Scarborough, J.; Waters, L. *J. Chem. Soc.* **1926**, 557–560.

Kinetics of the decomposition of **1c** in acetate buffers were also monitored by HPLC methods using 7:3 buffered MeOH/H_2O as eluant. Initial concentration of **1c** was 2.0×10^{-5} M in these studies. Kinetic simulations were performed with the MIREAK[33] software on an IBM PS/2 Model 50Z equipped with 1 megabyte of RAM and an 80287 math coprocessor.

The kinetics of the phenyl migration in **1a** and **1c** were performed in dry CH_2Cl_2 containing 1.4×10^{-4} M CF_3CO_2H at 25.0 °C. Kinetic data were gathered by monitoring the changes in UV absorbance at 310 and 316 nm of solutions containing either **1a** or **1c**. Wavelength scans were taken in the range of 300–350 nm, and the change in absorbance at the two wavelengths was recorded. Kinetic measurements were taken every 3.0 min for **1c** and every 10.0 min for **1a** for 2 half-lives.

A stock solution for **1a** (ca. 3.0×10^{-4} M) and **1c** (ca. 2.2×10^{-4} M) was prepared in dry CH_2Cl_2 and stored under N_2. To assure a constant concentration of acid, a new stock solution of 8.5×10^{-3} M CF_3CO_2H was prepared prior to each kinetic measurement. A 10-mL volumetric flask was evacuated with nitrogen, and CF_3CO_2H (10.0–10.7 mg) was added via syringe. The exact weight of dry CH_2Cl_2 to prepare an 8.5×10^{-3} M solution was then calculated and added via syringe, and the solution was kept under nitrogen prior to use. Each kinetic run was prepared by the addition of the *p*-benzoquinol imine stock solution (3.0 mL) with a graduated pipet to a dry UV cell, followed by the addition of an 8.5×10^{-3} M CF_3CO_2H solution (50 μL with a precalibrated 250-μL syringe) to give an acid solution concentration of 1.4×10^{-4} M. The UV cell was capped with a glass stopper, shaken vigorously for approximately 10 s, and placed in the thermostated UV cell holder for the remainder of the kinetic run.

Product Analyses. Identities of reaction products obtained from the decomposition of **1a–c** and **4** in aqueous solution were confirmed by HPLC comparison to authentic materials and by ^{1}H NMR comparison of authentic materials to product mixtures obtained from the decomposition of **1a–c** and **4** in D_2O solutions. Quantification of reaction products was performed by triplicate HPLC runs (20-μL injections) on the same solutions used for the UV kinetic runs. Buffered 6:4 MeOH/H_2O was used as the eluant. Extinction coefficients were determined by injection of appropriate solutions of authentic materials.

Products of the reaction of **1a** and **1c** in TFA/CH_2Cl_2 were determined under the same conditions employed in the kinetic studies with the exception of higher imine concentrations (ca. 0.01 M).

(33) Copyright 1984, Kenneth A. Wilde, 3604 Laurel Ledge Lane, Austin, TX 78731.

NMR Studies. The decomposition of **4** was monitored by ^{1}H NMR spectroscopy in 1:9 0.05 M KD_2PO_4/K_2DPO_4 buffer (pD 8.90, uncorrected) at 20 °C. A concentration of **4** of ca. 0.6 mM was obtained by injection of a 0.02 M solution (15 μL) of **4** in CD_3CN into the buffer (0.5 mL) which had previously been incubated in the NMR probe for ca. 20 min. The solvent peak was suppressed by standard methods during automatic data collection. DSS was added to the reaction mixture at completion to calibrate chemical shifts.

Similar procedures were used for the reaction of **1c** in 1:1 0.05 M AcOD/KOAc buffer (pD = 5.18, uncorrected) at 0 °C and a 1:1 0.05 M KD_2PO_4 buffer (pD = 7.36, uncorrected) at 20 °C. The initial concentration of **1c** present in the reaction mixtures was ca. 0.2 mM. A Bruker ACF 300-MHz NMR equipped with a variable temperature probe was used in all of these studies.

pK_a Determinations. The pK_a of the conjugate acids **19a,b** were determined under conditions identical to the kinetic studies by spectrophotometric titration methods that have been described elsewhere.[8] Absorbance vs pH data were collected at 256 nm for **19a** and 252 nm for **19b** in 2×10^{-5} M solutions of the imines. Total absorbances were ca. 0.035 AU for **19a** and ca. 0.05 AU for **19b**. The standard deviation of fit of the experimental data to the theoretical titration curve was ±0.002 AU in both cases.

Acknowledgment. The research at The Ohio State University was supported by Grant GM 36592-04 from the National Institutes of Health. The research at Miami University was supported, in part, by grants from the American Cancer Society (Nos. CN-23I and CN-23J). The 300-MHz NMR spectra were obtained at Miami University with equipment funded by NSF Grant No. CHE-9012532. Electron ionization high-resolution mass spectra were obtained at the Ohio State University Chemical Instrumentation Center, and high-resolution FAB spectra were obtained by Dr. Carolyn Cassidy at Miami on a Bruker CMS-47X FT-IRC spectrometer funded by the Ohio Board of Regents Academic and Research Challenge Programs.

Supplementary Material Available: The details of the kinetics of phenyl migration in **1a** and **1c**, Tables III–X, and NMR spectra for all compounds reported in the text (41 pages). This material is contained in libraries on microfiche, immediately follows this article in the microfilm version of the journal, and can be ordered from the ACS; see any current masthead page for ordering information.